

Supporting information

Impact of electrostatics on the adsorption of microgels at the interface of Pickering emulsions

Pascal Massé¹, Elisabeth Sellier³, Véronique Schmitt^{2}, Valérie Ravaine^{1*}*

¹Univ. Bordeaux, Institut des Sciences Moléculaires, ENSCBP, 16 Avenue Pey Berland, 33607 Pessac Cedex, France

²Univ. Bordeaux, Centre de Recherche Paul Pascal, 115 Avenue Dr Albert Schweitzer, 33600 Pessac, France

³ PLACAMAT, Université de Bordeaux, 87 avenue Dr Albert Schweitzer, 33608 Pessac, France

Content

I. Materials and methods

S1. TEM images of pNIPAM-co-AAc10% and pNIPAM-co-VAA5% microgels.

S2. Schematic description of front edge and side view of an adhesive film.

S3. Microscopy images of emulsion drops obtained with different concentrations of microgels.

II. Complementary results

S4. Temperature dependence of the hydrodynamic diameter in 0.01 M NaCl solution (pH~6) for 4 different microgels.

S5. Position of the mass centers of the microgels pNIPAM-co-AAc and the corresponding radial distribution functions.

S6. CryoSEM images of oil drop covered pNIPAM-co-VAA5% in the presence of NaCl.

S7. Position of the mass centers of the microgels pNIPAM-co-VAA and the corresponding radial distribution functions.

S8. Influence of pH on the stability of emulsions with pNIPAM-co-VAA.

III. Estimation of the charges of the microgels

I. MATERIALS AND METHODS

1. Particle characterization

Particle sizes and polydispersity index were determined by dynamic light scattering (DLS) with a Zetasizer Nano S90 Malvern Instruments equipped with a HeNe laser at 90°. Hydrodynamic diameters were calculated from diffusion coefficient using the Stokes-Einstein equation. All correlogram analyses were performed with the software supplied by the manufacturer. The polydispersity index is given by the cumulant analysis method.

The particles were also characterized using transmission electronic microscopy (TEM) in order to visualize their morphology and to check their monodispersity (Figure S1). A drop of diluted suspension was deposited on a copper grid covered by a carbon membrane. The electronic contrast of microgels was enhanced by labelling with uranyle acetate.

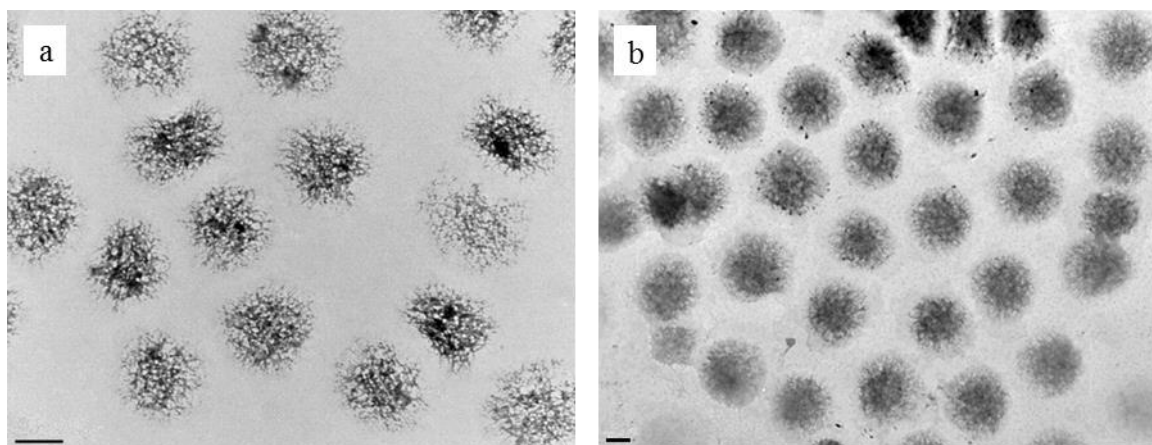


Figure S1. TEM images of pNIPAM-co-AAc10% (a), pNIPAM-co-VAA5% (b). Scale bar is 0.5 μm for both images.

Electrophoretic mobility measurements were carried out using the Zetasizer Nano ZS (from Malvern Instruments, UK) at the appropriate temperature, pH and ionic strength after allowing the mixture to equilibrate for 10 min. Each value results from at least 5 cycles of 15

measurements each.

The polymer content C_p (in $\text{g}\cdot\text{cm}^{-3}$) in aqueous dispersions was determined by the drying method. A known amount of the dispersion is first dried at a temperature higher than 50°C and then weighted to determine the mass of polymer and bound water. Following the work published by Lele *et al.*¹ it was considered that a particle is composed of 71 wt.% of polymer and 29 wt.% of bound water at 50°C . From the hydrodynamic particle diameter, $d_{H \text{ at } 50^\circ\text{C}}$, measured by DLS at 50°C , the particle number $n_{\text{particles}}$ was estimated as:

$$n_{\text{particles}} = \frac{6m_{\text{polymer}}}{\pi(d_{H \text{ at } 50^\circ\text{C}})^3} \left(\frac{1}{\rho_{\text{polymer}}} + \frac{0.29}{0.71\rho_{\text{water}}} \right) \quad (1)$$

where $\rho_{\text{polymer}}=1.269 \text{ g}\cdot\text{cm}^{-3}$, and $\rho_{\text{water}}=0.988 \text{ g}\cdot\text{cm}^{-3}$ are respectively the polymer and water densities.

2. Emulsion characterization

i) Drop size distribution determination by optical microscopy

The size distribution of emulsions was estimated by direct imaging using inverted optical microscope (Zeiss Axiovert X100) and video camera. Images were recorded and the dimensions of about 50 droplets were measured, so that both the surface average diameter D and the polydispersity P , defined by equation (2), could be estimated.

$$D = \frac{\sum_i N_i D_i^3}{\sum_i N_i D_i^2} \quad P = \frac{1}{D_m} \frac{\sum_i N_i D_i^3 |D_m - D_i|}{\sum_i N_i D_i^3} \quad (2)$$

where N_i is the total number of droplets with diameter D_i , D_m is the median diameter, *i.e.* the diameter for which the cumulative undersized volume fraction is equal to 50%.

ii) Quantification of drop adhesion

The flocculated state of emulsions was macroscopically and directly perceived by the observation of the emulsion flow behavior when the vial was tilted. If drops were well dispersed, the emulsion behaved as a liquid since the oil volume fraction was equal to 35% well below the random close packing. In the opposite, flocculated emulsions exhibited a plug flow, easily recognizable qualitatively. In order to quantify the flocculation extent, we applied the method already described elsewhere for both surfactant-stabilized²⁻⁴ or Pickering emulsions⁵. It consists in measuring the non-zero angle θ_{adh} formed between two adhesive drops (Figure S2).

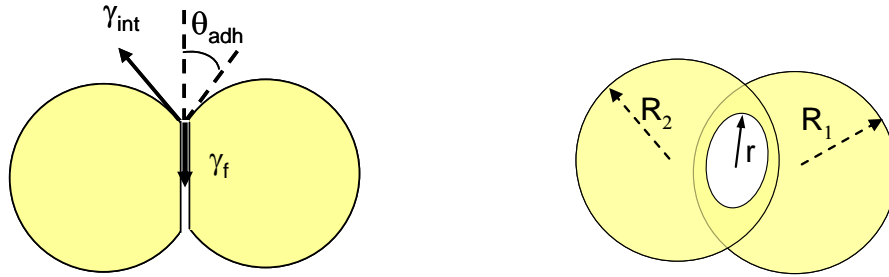


Figure S2. Front edge and side view of an adhesive film (adapted from²)

This angle results from the formation of a flat film between two neighboring drops which interact through both attraction and short-range repulsion forces. As schematically drawn in Fig. S2, the adhesion angle can be experimentally determined by observing adhesive drops. Indeed, when observed from side view, the flat film appears as a white ellipse (Fig. S1b). The adhesion angle can therefore be estimated by measuring the radius of two adhesive droplets, R_1 and R_2 , and the radius of the adhesive film between the droplets, r (corresponding to the large axis of the ellipse), through the following relation:

$$2\theta_{adh} = \text{Arcsin}\left(\frac{r}{R_1}\right) + \text{Arcsin}\left(\frac{r}{R_2}\right) \quad (3)$$

iii) Characterization of microgel adsorption through limited coalescence

Limited coalescence arises in Pickering emulsions where particles are irreversibly anchored at the oil–water interface⁶⁻⁸. If the system is emulsified with a low amount of particles, the newly created droplets are insufficiently protected by the particles. When the agitation is stopped, the droplets coalesce, thus reducing the total amount of oil–water interface. Since the particles are irreversibly adsorbed, the coalescence process stops as soon as the oil–water interface is sufficiently covered and the resulting emulsions exhibit remarkably narrow size distributions ($P < 30\%$)⁸. The final surface area of the droplets depends on the initial amount of particles and on their arrangement at the interface. For emulsions undergoing limited coalescence, the final interfacial particle coverage can be directly deduced from the surface average drop size, D . Indeed, the total interfacial area S_{int} of the emulsion is directly linked to D ($S_{int} = 6V_d/D$, where V_d is the oil volume). Assuming that all the particles are adsorbed, the interface area that the particles may cover is estimated from their equatorial section $S_{eq} = n_{particles} \pi (d_{H \text{ at } 25^\circ C} / 2)^2$, where $n_{particles}$ is the total number of particles deduced from Eq. 1 and $d_{H \text{ at } 25^\circ C}$ is their hydrodynamic diameter at $25^\circ C$. The surface coverage, C , defined as $C = S_{eq} / S_{int}$ can thus be estimated after measuring D :

$$\frac{1}{D} = \frac{n_{particles} \pi d_{H \text{ at } 25^\circ C}^2}{24 C V_d} = \frac{S_{eq}}{6 C V_d} \quad (4)$$

Equation 4 shows that the surface coverage characterizing the particle packing at the interface can directly be deduced from a drop size measurement in the low particle concentration regime where the average inverse droplet diameter is proportional to S_{eq} / V_d .

An example of limited coalescence process obtained with pNIPAM-co-AAc 10% is shown in Figure S3.

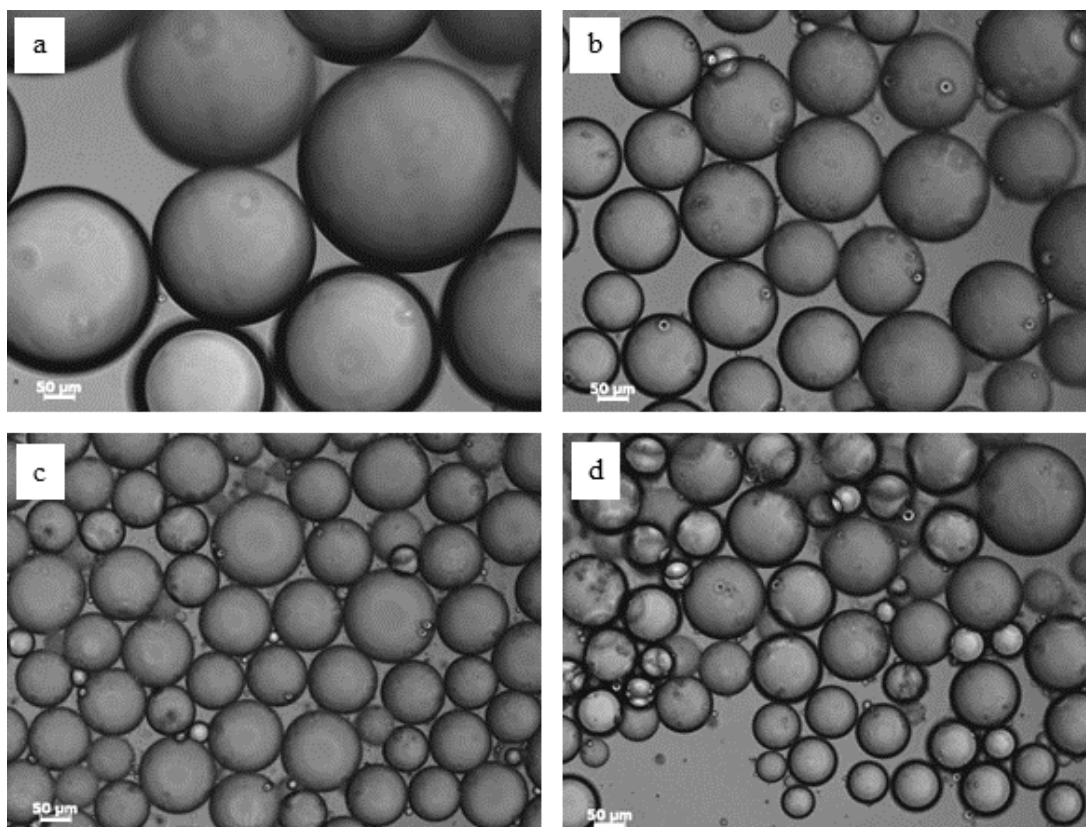


Figure S3. Microscopy images of emulsion drops obtained with different pNIPAM-co-AAc10% microgels concentrations (0.01, 0.02, 0.03, 0.04 wt%, from (a) to (d) respectively). Conditions: pH~6, deionized water, T=25°C.

iv) Cryo-SEM observations

Cryo-SEM observations were carried out with a JEOL 6700FEG electron microscope equipped with liquid nitrogen cooled sample preparation and transfer units. A small amount of emulsion was first deposited on the aluminium specimen holder. The sample was frozen in the slushing station with boiling liquid nitrogen. The specimen was transferred under vacuum from the slushing station to the preparation chamber. The latter was hold at T=-150°C and P=10⁻⁵ Pa and was equipped with a blade used to fracture the sample. Once fractured, the sample was coated by a layer of Au-Pd and was then inserted into the observation chamber equipped with a SEM stage cold module hold at -150°C. Dodecane has a low melting

temperature (-9.6°C) that avoided oil crystallization during the freezing step. Moreover dodecane was amorphous in the solid state, so the droplet interfaces remained spherical and smooth. Heptane was also used when light sublimation of the specimen was required. In this case, after fracturing the sample, the temperature in the preparation chamber was raised to -95°C during less than 5 min before decreasing again the temperature and then inserting the sample into the observation chamber. From image analysis, we can determine the center-to-center distance, d_{CC} , and the coverage C , defined as:

$$C = \frac{\frac{3}{4}\pi(d_{H25^\circ C})^2}{\frac{3\sqrt{3}}{2}(d_{CC})^2} \quad (5)$$

Edge-view of thin films separating two oil drops corresponding to Figure S2 can be obtained by cryo-SEM experiments; these images allow another determination of the adhesion angle between drops and therefore a quantification of flocculation.

II. Complementary results

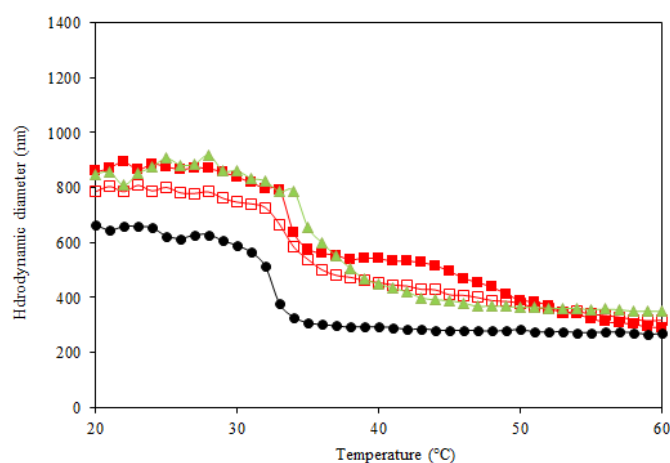


Figure S4. Temperature dependence of the hydrodynamic diameter in 0.01 M NaCl solution (pH~6) for 4 different microgels: pNIPAM (dark circles), pNIPAM-co-AAc5% (red full squares), pNIPAM-co-AAc10% (red empty squares), pNIPAM-co-VAA5% (green triangles).

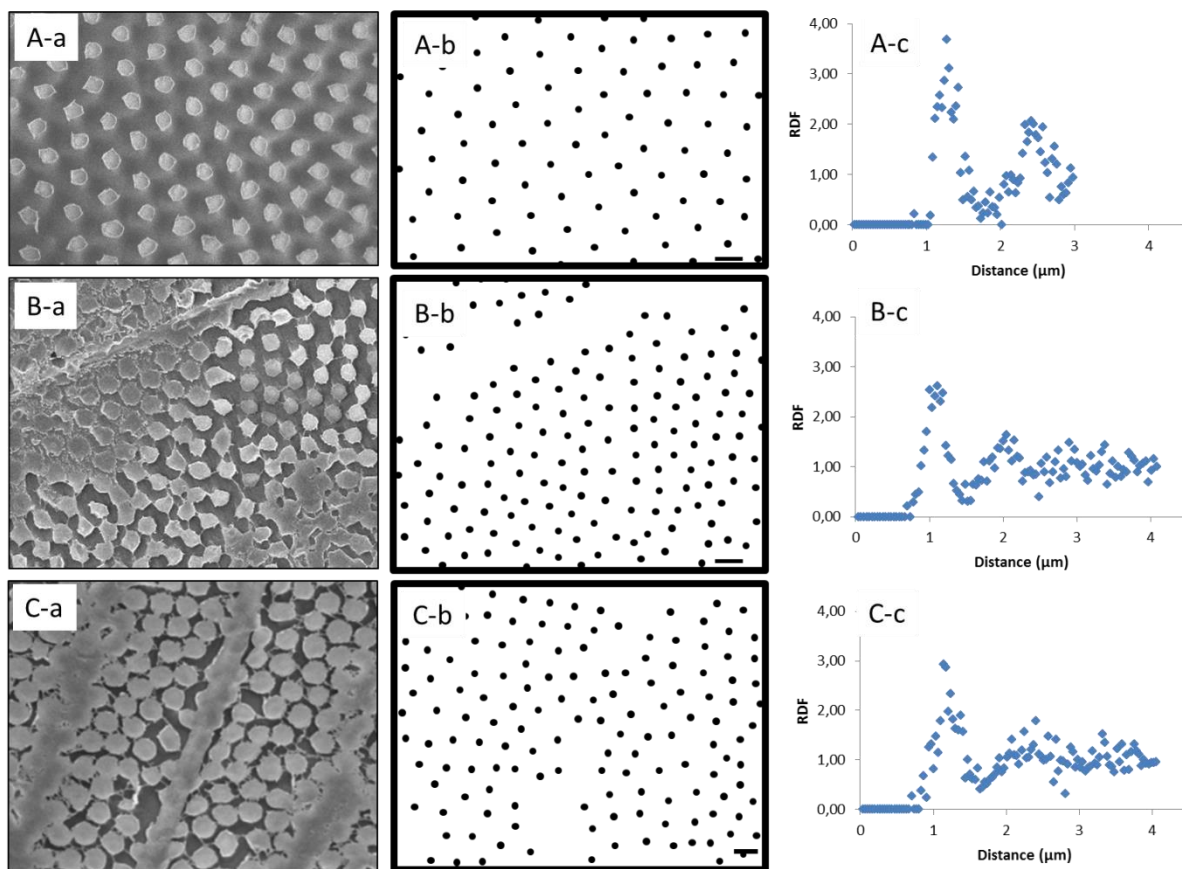


Figure S5. CryoSEM images of adsorbed microgels (a) and their corresponding binary images where only the microgel mass centers are represented (b), followed by the radial distribution function (RDF) (c). Samples : pNIPAM-co-AAc5%, pH=6, T=25°C (A), pNIPAM-co-AAc10%, pH=6, T=25°C (B), pNIPAM-co-AAc10%, pH=6, [NaCl]=0,01M, T=25°C (C). The scale bar is 1 μm . The oil is heptane. Images A, B and C correspond to figure 5 a, c and d.

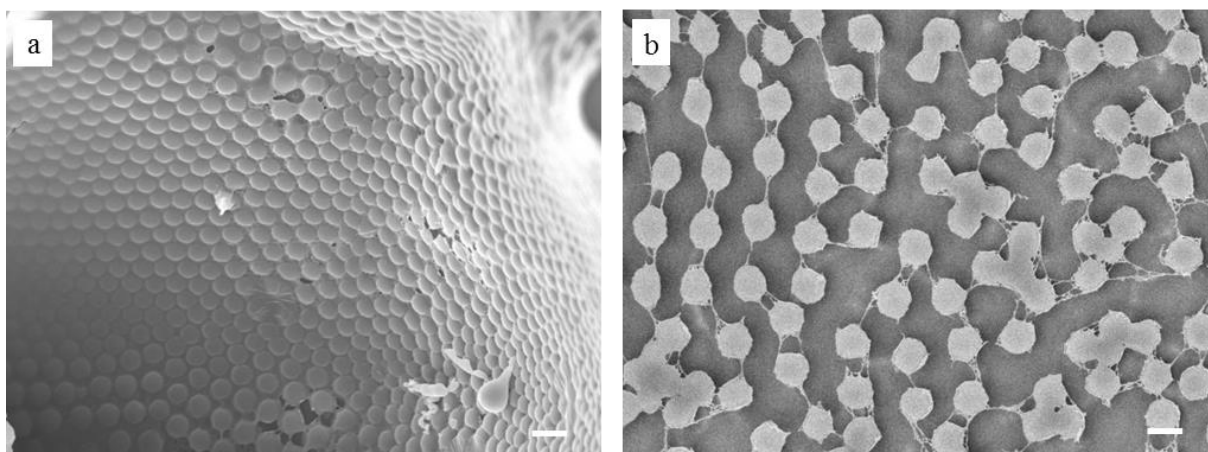


Figure S6. CryoSEM of oil drop covered with microgels : a) pNIPAM-co-VAA5% microgels ($C_p=0.014$ wt%), $T=25^\circ\text{C}$, $\text{pH}=6$, $[\text{NaCl}]=0.01\text{M}$; b) pNIPAM-co-VAA5% microgels ($C_p=0.014$ wt%), $T=4^\circ\text{C}$, $\text{pH}=6$, $[\text{NaCl}]=0.01\text{M}$. The oil is dodecane for image (a) or heptane for (b). Scale bar is $1\ \mu\text{m}$ for all images.

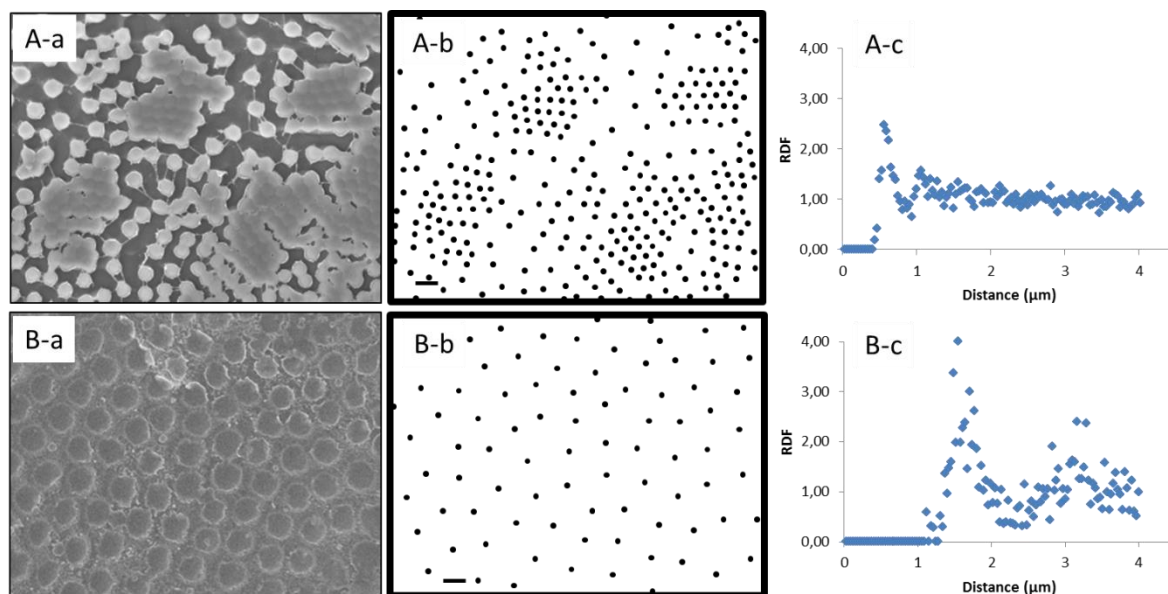


Figure S7. CryoSEM images of adsorbed microgels (a) and their corresponding binary images where only the microgel mass centers are represented (b), followed by the radial distribution function (c). Samples : pNIPAM-co-VAA5%, $\text{pH}=6$, $T=25^\circ\text{C}$ (A), pNIPAM-co-VAA5%, $\text{pH}=6$, $T=4^\circ\text{C}$ (B). The scale bar is $1\ \mu\text{m}$. The oil is heptane. Images A and B correspond to figure 6 a and b.

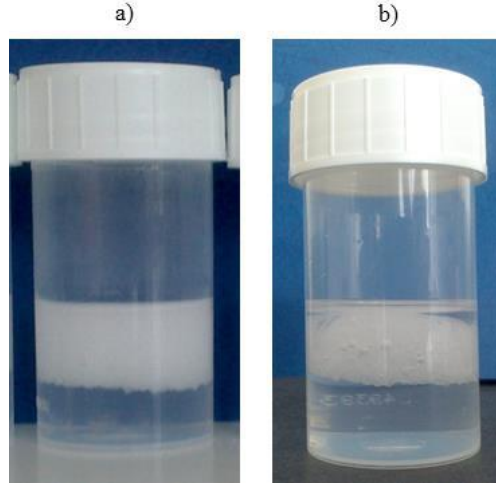


Figure S8. Oil-in-water emulsions stabilized with pNIPAM-co-VAA 5% microgels ($C_p=0.015$ wt%), $T=25^\circ\text{C}$, observed after 5 hours: a) $\text{pH}=6$; b) $\text{pH}=3$.

III. Estimation of the charges of the microgels

Ohshima's theory gives a relation between the measurable electrophoretic mobility of a soft core-shell particle and the charge density ρ of the polyelectrolyte shell. The electrophoretic mobilities of the microgels were determined experimentally in different pH conditions, in $[\text{KCl}]=10^{-3}\text{M}$, at 25°C . To make use of equation (1) given in the manuscript, various parameters have to be calculated.

κ_m , the Debye-Hückel parameter of the shell, is related to κ the Debye-Hückel parameter via relation (6)

$$\kappa_m = \kappa \left[1 + \left(\frac{\rho}{2ze n^\infty} \right)^2 \right]^{1/4} \quad (6)$$

where z is the valence of the symmetrical electrolyte (1 in our case), e the elementary charge, n^∞ is the bulk electrolyte concentration, expressed in number of ions/ m^3 .

ψ_{DON} the Donnan potential in the shell is calculated according to equation (7) and ψ_0 the surface potential according to equation (8):

$$\psi_{DON} = \frac{kT}{ze} \ln \left[\frac{\rho}{2zen^\infty} + \left\{ \left(\frac{\rho}{2zen^\infty} \right)^2 + 1 \right\}^{1/2} \right] \quad (7)$$

$$\psi_0 = \frac{kT}{ze} \left(\ln \left[\frac{\rho}{2zen^\infty} + \left\{ \left(\frac{\rho}{2zen^\infty} \right)^2 + 1 \right\}^{1/2} \right] + \frac{2zen^\infty}{\rho} \left[1 - \left\{ \left(\frac{\rho}{2zen^\infty} \right)^2 + 1 \right\}^{1/2} \right] \right) \quad (8)$$

where k is the Boltzmann constant and T is the absolute temperature (298K).

The softness parameter $1/\lambda$ is chosen as $8 \cdot 10^9 \text{ m}^{-1}$, as estimated previously for pNIPAM microgels⁹. Even if this parameter should slightly depend on the swelling degree of the microgels, it was verified that a factor 5 poorly affected the value of μ (less than 1% of variation).

Once ρ the volume charge density was determined by matching the theoretical value of μ to the experimental one, it was converted to the concentration of charges per microgel, which in turn was compared to the number of monomeric units per microgels. This latter was estimated with the assumption that a particle is composed of 71 wt.% of polymer and 29 wt.% of water at 50°C¹.

References

1. Lele, A. K.; Hirve, M. M.; Badiger, M. V.; Mashelkar, R. A. Predictions of bound water content in poly(N-isopropylacrylamide) gel. *Macromolecules* **1997**, *30* (1), 157.
2. Leal-Calderon, F.; Schmitt, V.; Bibette, J. *Emulsion Science. Basic Principles. 2nd version*; Springer ed.2007.
3. Poulin, P.; Bibette, J. Wetting of emulsions droplets: From macroscopic to colloidal scale. *Phys. Rev. Lett.* **1997**, *79* (17), 3290-3293.
4. Aronson, M. P.; Princen, H. M. Contact angles in oil-in-water emulsions stabilized by ionic surfactants. *Colloids Surf.* **1982**, *4* (2), 173-184.

5. Destribats, M.; Lapeyre, V.; Sellier, E.; Leal-Calderon, F.; Ravaine, V.; Schmitt, V. Origin and control of adhesion between emulsion drops stabilized by thermally sensitive soft colloidal particles. *Langmuir* **2012**, 28 (8), 3744-3755.
6. Whitesides, T. H.; Ross, D. S. Experimental and Theoretical Analysis of the Limited Coalescence Process: Stepwise Limited Coalescence. *J. Colloid Interface Sci.* **1995**, 169 (1), 48.
7. Arditty, S.; Whitby, C. P.; Binks, B. P.; Schmitt, V.; Leal-Calderon, F. Some general features of limited coalescence in solid-stabilized emulsions. *Eur. Phys. J. E* **2003**, 11 (3), 273.
8. Arditty, S.; Schmitt, V.; Giermanska-Kahn, J.; Leal-Calderon, F. Materials based on solid-stabilized emulsions. *J. Colloid Interface Sci.* **2004**, 275 (2), 659.
9. García-Salinas, M. J.; Romero-Cano, M. S.; De Las Nieves, F. J. Colloidal stability of a temperature-sensitive poly(N-isopropylacrylamide/2-acrylamido-2-methylpropanesulphonic acid) microgel. *J. Colloid Interface Sci.* **2002**, 248 (1), 54-61.